On-chip engineering of high-dimensional path-entangled states in a quadratic coupled-waveguide system

Xiang-Wen Luo,[1,*] Qun-Yong Zhang,[2,*] Ping Xu,[1,3,†] Rong Zhang,[1] Hua-Ying Liu,[1] Chang-Wei Sun,[1] Yan-Xiao Gong,[1] Zhen-Da Xie,[1,4] and Shi-Ning Zhu[1]

[1]*National Laboratory of Solid State Microstructures and School of Physics, Nanjing University, Nanjing 210093, People's Republic of China*
[2]*Faculty of Mathematics and Physics, Huaiyin Institute of Technology, Huaian 223003, People's Republic of China*
[3]*Institute for Quantum Information and State Key Laboratory of High Performance Computing, College of Computing,
National University of Defense Technology, Changsha 410073, People's Republic of China*
[4]*National Laboratory of Solid State Microstructures and School of Electronic Science and Engineering, Nanjing University,
Nanjing 210093, People's Republic of China*

High-dimensional quantum entangled states are a highly desired resource for their extended possibilities in quantum information processing. In this paper, we introduce on-chip engineering of a variety of path-entangled states based on the simultaneous enabling of spontaneous parametric down-conversion and efficient coupling between waveguides in a quadratic coupled-waveguide system. By varying the properties of pump beams, the phase-matching conditions, and the coupling coefficients in a three-coupled-waveguide system, it is possible to generate the deterministic and robust three-path biphoton entangled states without any postprocessing, as well as to transform the output photons among different types of path entanglement. This integrated implementation of the entanglement source will become an important building block for practical applications of on-chip quantum technologies.

I. INTRODUCTION

Quantum entanglement is a vital physical resource in quantum information science which includes quantum computation, quantum communication, quantum metrology, and fundamental physics in quantum mechanics [1]. One of the most common methods for generating the source of entangled photon pairs is to use the nonlinear optical process of spontaneous parametric down-conversion (SPDC). In SPDC, photons from a pump laser beam, within a nonlinear optical medium, can spontaneously be converted into signal-idler photon pairs that are momentum and energy conserved. Entangled states of a high-dimensional system, which endow each photon with more shared information, are of particular interest due to their extended capabilities [2]. They enable the realization of various quantum communication schemes that can offer higher-density coding and greater resilience to errors in quantum computation [3,4]. High-dimensional entangled states are an essential step for a deeper understanding of quantum information processing and the foundations of quantum mechanics. They have been realized by encoding in many degrees of freedom, such as longitudinal momentum [5], frequency domain [6], and orbital angular momentum [7], etc.

Naturally, as path-encoded quantum states are used, scalability and phase stability become great challenges for the

traditional bulk optical approach in many quantum optical experiments. An overwhelming solution is to develop integrated photonic circuits which have become outstanding platforms for various quantum technologies, including nonclassical state generation [8,9], on-chip quantum devices [10–12], and quantum information processing applications [13,14]. To harness the path degree of freedom, integrated optical circuits are usually built upon various architectures of directional couplers which can be realized by designing closely adjacent waveguides. By virtue of the coupling between adjacent channels, a single photon launched into one of the waveguides can be gradually distributed across the array. Gräfe *et al.* reported on-chip generation of high-order *W* states by manipulating the dynamic evolution of single photons in an evanescently coupled linear waveguide system [15], but their photons are generated externally to the array by using bulk photonic elements before importing into the chip. Perez-Leija *et al.* proposed a convenient method to generate photon-encoded *W* states in multiport waveguide-array systems and demonstrated the perfect transfer of path-entangled photons in these fully integrable optical arrangements [16,17]. Nonlinear waveguide arrays have also been widely explored as attractive platforms for they can combine SPDC processes and quantum walks in a single chip [18–20]. They further open the possibility for the investigation of high-dimensional quantum states in a fully integrated device. Solntsev *et al.* experimentally demonstrated the simultaneous generation of correlated photon pairs which reveal unique spatial correlations and their quantum walks inside a nonlinear waveguide array [21]. However, these investigations mainly focused on the properties of quantum

---

*The first two authors contributed equally to this work.
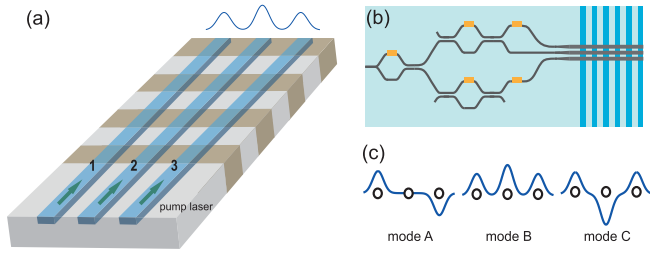†Corresponding author: pingxu520@nju.edu.cn

FIG. 1. (a) Schematic diagram of the coupled-waveguide system containing three parallel nonlinear waveguides. (b) The complete system contains the pump multiplexer, the taper region, and the three-coupled-waveguide system. (c) The transverse modal field of the waveguide system corresponds to three different eigenmodes.

walks rather than on the preparation of specific entangled states. Until recently, Kruse *et al.* demonstrated a two-in-one waveguide source allowing for a robust two-photon NOON state preparation when pumped into a single waveguide [22]. Wu *et al.* proposed a scheme for the generation of Bell states in a system incorporating two coupled quadratic nonlinear waveguides [23]. Setzpfandt *et al.* experimentally demonstrated the generation of split states, robust NOON states, and various intermediate regimes on a single chip driven by two classical pump beams with a variable phase difference [24,25]. Yang *et al.* theoretically investigated the transformation of different types of path-entangled states by modulating the $\chi^{(2)}$ distributions in a SPDC array [26]. To our knowledge, in all schemes to date, it is not yet known how to produce and manipulate versatile high-dimensional path-entangled states, such as the *W* state or the Dicke state, which underlie the keystones of on-chip quantum information processing. So in this article we theoretically study the unique and reconfigurable generation of path-entangled states in high dimensions but with a limited number of quadratic coupled-waveguide systems. This moderate scale of coupled-waveguide systems is frequently used to prepare the initial quantum states for the cascaded quantum information processing.

This article is organized as follows. We give the description of our device and derive the fully expanded expression of a high-dimensional entangled state based on the eigenmode basis in Sec. II. In Sec. III, we discuss manipulation of the high-dimensional entangled state in a coupled-waveguide system. In Sec. IV, we calculate the genuine multipartite entanglement concurrence to quantify the high-dimensional entanglement. Conclusions are given in Sec. V.

II. THREE-COUPLED-WAVEGUIDE SYSTEM

We begin from the three-coupled-waveguide system shown in Fig. 1(a) which can be described by coupled-mode theory under a weak-coupled condition and an ignorable next-nearest-neighboring coupling. The substrate material can be one of the quadratic nonlinear crystal with strong second-order nonlinearity and the capability for ferroelectric poling, such as LiNbO$_3$ (LN) or LiTaO$_3$ (LT). Three pump beams are designed to originate from one single injected pump by an on-chip $1 \times N$ beam-splitting network as shown in Fig. 1(b), whose architecture consists of cascaded Mach-Zehnder interferometers [27], and thus the relative amplitude and phase

among the three waveguides can be precisely controlled. The pump beam-splitting network is designed to be single mode waveguides for the pump and a taper is cascaded to transform into a wider single-mode waveguide but for the down-converted photons.

Additionally, in our design we apply domain engineering in the three-coupled waveguide region so as to introduce a periodic poling with the proper length for the efficient generation of entangled photon pairs, which is widely used in quasi-phase-matching (QPM) nonlinear optics [28,29]. The poling period is designed to match the phase mismatch between the fundamental modes of the pump, the signal, and the idler. The signal-idler photon pairs are generated from the QPM SPDC, and they can hop between the neighboring waveguides due to evanescent coupling characterized by the coupling coefficient κ, which is determined by the distance between two adjacent waveguides and the operating wavelength of the device. In degenerate SPDC, the pump frequency is twice that of the degenerate down-converted photons; it is commonly designed so that only the down-converted photons are affected by the coupling geometry and will result in a two-photon quantum walk while the pump photons remain uncoupled. At the end face of this quadratic coupled-waveguide system, the entangled photon source can be combined with cascaded integrated waveguide circuits for further quantum information processing.

Under the weak-coupling assumption, the coupled-mode equations for the single mode of the classical light field in this system can be written as [30]

$$\frac{dE_1}{dz} = -i\beta_1 E_1 + i\kappa_{12}E_2,$$
$$\frac{dE_2}{dz} = -i\beta_2 E_2 + i\kappa_{21}E_1 + i\kappa_{23}E_3, \qquad (1)$$
$$\frac{dE_3}{dz} = -i\beta_3 E_3 + i\kappa_{32}E_2,$$

where E_i ($i = 1, 2, 3$) represent the mode amplitudes of the electric field in the corresponding waveguide i, β_i are the propagation constants along the z axis, and κ_{ij} represent the coupling coefficients between adjacent waveguides i and j. In the case of codirectional coupling, conservation of energy calls for $\kappa_{ij} = \kappa_{ji}$. For simplicity, we assume all the waveguides are identical and regularly arrayed, i.e., $\beta_1 = \beta_2 = \beta_3 = \beta_0$ and $\kappa_{12} = \kappa_{21} = \kappa_{23} = \kappa_{32} = \kappa$. According to the coupled-mode analysis, the system eigenmodes can be expressed as the superposition of the electric field in each waveguide,

$$\tilde{E} = u_1(\vec{\rho})E_1(z) + u_2(\vec{\rho})E_2(z) + u_3(\vec{\rho})E_3(z), \qquad (2)$$

where $u_i(\vec{\rho})$ represent the transverse field distributions in waveguide i. The longitudinal electric field satisfies the eigenvalue equation $d\tilde{E}/dz = -i\beta\tilde{E}$. If we substitute these formulas into Eq. (1) and keep the equation true at arbitrary $u_i(\vec{\rho})$, we can get the eigenvalues of the corresponding propagation constants in the three-coupled-waveguide system as

$$\beta_A = \beta_0, \quad \beta_B = \beta_0 - \sqrt{2}\kappa, \quad \beta_C = \beta_0 + \sqrt{2}\kappa. \quad (3)$$

The subscripts *A*, *B*, and *C* represent the three different eigenmodes of the system which are shown in Fig. 1(c).

Then the corresponding electric fields of these eigenmodes can be rewritten as

$$\tilde{E}_A = u_A(\vec{\rho})e^{i\beta_A z} = \frac{1}{\sqrt{2}}[u_1(\vec{\rho}) - u_3(\vec{\rho})]e^{i\beta_A z},$$

$$\tilde{E}_B = u_B(\vec{\rho})e^{i\beta_B z} = \frac{1}{2}[u_1(\vec{\rho}) + \sqrt{2}u_2(\vec{\rho}) + u_3(\vec{\rho})]e^{i\beta_B z}, \quad (4)$$

$$\tilde{E}_C = u_C(\vec{\rho})e^{i\beta_C z} = \frac{1}{2}[u_1(\vec{\rho}) - \sqrt{2}u_2(\vec{\rho}) + u_3(\vec{\rho})]e^{i\beta_C z},$$

where $u_A(\vec{\rho})$, $u_B(\vec{\rho})$, and $u_C(\vec{\rho})$ represent the transverse field distribution of each eigenmode.

In the case of individual waveguides, the presence of two photons, one photon, and no photon at a given output site corresponds to the states of $|2\rangle$, $|1\rangle$, and $|0\rangle$, respectively. The full Hamiltonian of the three-coupled waveguide system can be expressed by a linear part given by the free propagation and the coupling behavior of the fields, as well as a nonlinear interaction part describing the SPDC process. To derive the generated biphoton state in the poled coupler system, we can write the effective Hamiltonian in the interaction picture as

$$\hat{H}_I = \varepsilon_0 \int_V dV \chi^{(2)} E_p^{(+)} \hat{E}_s^{(-)} \hat{E}_i^{(-)} + \text{H.c.}, \quad (5)$$

where ε_0 is the vacuum permittivity, the integral is taken over the interaction volume V, and $\chi^{(2)}$ is the effective nonlinear coefficient of the medium. $E^{(+)}$ and $E^{(-)}$ are positive- and negative-frequency components of the field operators. The subscripts p, s, and i represent the pump, the signal, and the idler, respectively. H.c. denotes the Hermitian conjugate part. To calculate the effective Hamiltonian, we can express the fields in the eigenmode basis, and then the pump beam which can be treated as a classical wave can be expressed as

$$E_p^{(+)} = \sum_l \int d\omega_p \alpha(\omega_p) A_l^{(p)} u_l^{(p)}(\vec{\rho}) e^{-i\left[\beta_l^{(p)}z - \omega_p t\right]}, \quad (6)$$

where l is the eigenmode of the pump photon, and $\alpha(\omega_p)$ is the pump mode function which gives the energy-conservation condition. $A_l^{(p)}$ is the pump excitation amplitude, and $u_l^{(p)}(\vec{\rho})$ is the transverse field distribution of the pump photon. The signal and idler fields are usually treated quantum mechanically:

$$\hat{E}_s^{(-)} = \sum_m \int d\omega_s u_m^{(s)}(\vec{\rho}) e^{i\left[\beta_m^{(s)}z - \omega_s t\right]} \hat{a}_m^{(s)\dagger}, \quad (7)$$

and

$$\hat{E}_i^{(-)} = \sum_n \int d\omega_i u_n^{(i)}(\vec{\rho}) e^{i\left[\beta_n^{(i)}z - \omega_i t\right]} \hat{a}_n^{(i)\dagger}. \quad (8)$$

The subscripts m and n are the eigenmodes of signal and idler photons which can be any one in the set of $\{A, B, C\}$. $\hat{a}_{m(n)}^{\dagger}$ represent the creation operators in the eigenmode basis, which can be deduced from the waveguide basis $\hat{b}_i^{\dagger}$ $(i = 1, 2, 3)$ according to Eq. (4):

$$\hat{a}_A^{\dagger} = \frac{1}{\sqrt{2}}(\hat{b}_1^{\dagger} - \hat{b}_3^{\dagger}),$$

$$\hat{a}_B^{\dagger} = \frac{1}{2}(\hat{b}_1^{\dagger} + \sqrt{2}\hat{b}_2^{\dagger} + \hat{b}_3^{\dagger}), \quad (9)$$

$$\hat{a}_C^{\dagger} = \frac{1}{2}(\hat{b}_1^{\dagger} - \sqrt{2}\hat{b}_2^{\dagger} + \hat{b}_3^{\dagger}).$$

According to the first-order perturbation theory [31], by substituting Eqs. (6)–(8) into Eq. (5), we can obtain the biphoton state in the eigenmode basis as

$$|\psi\rangle^{\text{eig}} = \frac{1}{\sqrt{N}} \int d\omega_s \int d\omega_i \int d\vec{\rho} \int dz \alpha(\omega_p) \sum_{l,m,n} A_l^{(p)}$$
$$\times u_l^{(p)}(\vec{\rho}) u_m^{(s)}(\vec{\rho}) u_n^{(i)}(\vec{\rho}) e^{(i\Delta\beta_{lmn}z)} \hat{a}_m^{(s)\dagger} \hat{a}_n^{(i)\dagger} |0\rangle, \quad (10)$$

where N is a normalization constant, $\vec{\rho}$ is the integral area of transverse field components, and $\Delta\beta_{lmn} = \beta_l^{(p)} - \beta_m^{(s)} - \beta_n^{(i)} - G$ are the values of phase mismatch in the SPDC processes, where G is the reciprocal vector of the periodically poled region which can be carefully designed. We define the transverse field overlap between the pump photon and the down-converted photons as $\Phi = \int d\vec{\rho} u_l^{(p)}(\vec{\rho}) u_m^{(s)}(\vec{\rho}) u_n^{(i)}(\vec{\rho})$. According to Eq. (4), the transverse field overlap integral for any combination of three different eigenmodes can be deduced, and the results of the derivation which are multiples of the fixed value $\Phi_0 = \int d\vec{\rho} u^{(p)}(\vec{\rho}) u^{(s)}(\vec{\rho}) u^{(i)}(\vec{\rho})$ are listed in Table I, where $u^{(j)}(\vec{\rho})$ $(j = p, s, i)$ represent the transverse fields in an individual waveguide of pump, signal, and idler photons, respectively. The first line in Table 1 means l has three different pump eigenmodes A, B, and C. The left column and the last line in the table correspond to three different signal and idler eigenmodes, respectively. For instance, if all the pump, signal, and idler photons are in the eigenmodes A, i.e., $lmn = AAA$, then the result of the transverse field overlap integral will be 0. Otherwise if $lmn = AAB$, the result of the

TABLE I. Results of field overlap integral Φ for the pump, signal, and idler photons. l, m, and n represent the eigenmodes which can be any one in the set of $\{A, B, C\}$.

m \ l	A			B			C		
A	0	$\frac{1}{2}\Phi_0$	$\frac{1}{2}\Phi_0$	$\frac{1}{2}\Phi_0$	0	0	$\frac{1}{2}\Phi_0$	0	0
B	$\frac{1}{2}\Phi_0$	0	0	0	$\frac{1+\sqrt{2}}{4}\Phi_0$	$\frac{1-\sqrt{2}}{4}\Phi_0$	0	$\frac{1-\sqrt{2}}{4}\Phi_0$	$\frac{1+\sqrt{2}}{4}\Phi_0$
C	$\frac{1}{2}\Phi_0$	0	0	0	$\frac{1-\sqrt{2}}{4}\Phi_0$	$\frac{1+\sqrt{2}}{4}\Phi_0$	0	$\frac{1+\sqrt{2}}{4}\Phi_0$	$\frac{1-\sqrt{2}}{4}\Phi_0$
m \ n	A	B	C	A	B	C	A	B	C

overlap integral will be $\Phi_0/2$. Then the fully expanded expression of the biphoton state can be written as

$$|\psi\rangle^{\text{eig}} = U\Phi_0 \int d\omega_s \int d\omega_i \alpha(\omega_p) \left\{ A_A^{(p)} \left[\sin c\left(\frac{\Delta\beta_{AAB}L}{2}\right)\hat{a}_A^\dagger\hat{a}_B^\dagger + \sin c\left(\frac{\Delta\beta_{AAC}L}{2}\right)\hat{a}_A^\dagger\hat{a}_C^\dagger \right] + A_B^{(p)} \left[\frac{1}{2}\sin c\left(\frac{\Delta\beta_{BAA}L}{2}\right)\hat{a}_A^\dagger\hat{a}_A^\dagger \right. \right.$$

$$+ \frac{1+\sqrt{2}}{4}\sin c\left(\frac{\Delta\beta_{BBB}L}{2}\right)\hat{a}_B^\dagger\hat{a}_B^\dagger + \frac{1+\sqrt{2}}{4}\sin c\left(\frac{\Delta\beta_{BCC}L}{2}\right)\hat{a}_C^\dagger\hat{a}_C^\dagger + \frac{1-\sqrt{2}}{2}\sin c\left(\frac{\Delta\beta_{BBC}L}{2}\right)\hat{a}_B^\dagger\hat{a}_C^\dagger \right]$$

$$+ A_C^{(p)} \left[\frac{1}{2}\sin c\left(\frac{\Delta\beta_{CAA}L}{2}\right)\hat{a}_A^\dagger\hat{a}_A^\dagger + \frac{1-\sqrt{2}}{4}\sin c\left(\frac{\Delta\beta_{CBB}L}{2}\right)\hat{a}_B^\dagger\hat{a}_B^\dagger \right.$$

$$\left. \left. + \frac{1-\sqrt{2}}{4}\sin c\left(\frac{\Delta\beta_{CCC}L}{2}\right)\hat{a}_C^\dagger\hat{a}_C^\dagger + \frac{1+\sqrt{2}}{2}\sin c\left(\frac{\Delta\beta_{CBC}L}{2}\right)\hat{a}_B^\dagger\hat{a}_C^\dagger \right] \right\} |0\rangle. \tag{11}$$

In the above state, the slowly varying terms and constants are all absorbed into U. $A_A^{(p)}$, $A_B^{(p)}$, and $A_C^{(p)}$ are the excitation amplitudes of the pump light in modes A, B, and C, respectively. The properties of the generated photon pairs are determined by the pump excitation amplitudes and the sinc functions which depend on the phase mismatch $\Delta\beta_{lmn}$ of the SPDC processes and the length of the periodically poled region L. Different combinations of eigenmodes for the generated photon pairs yield different phase-matching conditions, as their propagation constants are modified uniquely. The state in Eq. (11) contains several distinct phase-matching conditions, which we can regarded as the different possibilities for distributing two SPDC photons across three eigenmodes. Due to their spectral separation, we can selectively excite different eigenmode combinations by choosing the proper pump wavelength, tuning the properties of the input pump laser, and adjusting the sample structure or the sample temperature; then different quantum states can be obtained. In the following we discuss manipulation of high-dimensional path-entangled states by exciting different SPDC processes.

III. MANIPULATION OF HIGH-DIMENSIONAL PATH-ENTANGLED STATES

In a SPDC process, a pump beam generates the signal and idler photons with the same polarization and half the pump frequency, it is usually called degenerate type-I or type-0 SPDC process in which the generated photon pairs are indistinguishable. In this section, we consider another situation, namely, the values of phase mismatch being degenerate. If the signal and idler photons are both in mode A, or one in mode B and the other in mode C, then the value of the phase mismatch will be $\Delta\beta_0$ as illustrated for modes AA, BC, CB in the white dashed box in Fig. 2. From this figure, we can see that both signal and idler photons have three different eigenmodes, their different combinations will lead to different values of phase mismatch. As the coupling of the pump laser is ignored, the mode of the pump beam is not taken into consideration. The SPDC process which generates two photons both in eigenmodes B will lead the value of phase mismatch to $\Delta\beta_0 + 2\sqrt{2}\kappa$, whereas the value of phase mismatch for the two photons in eigenmodes CC will be $\Delta\beta_0 - 2\sqrt{2}\kappa$. In the case that one photon is generated in mode A and the other in mode C, the value of the phase mismatch will be $\Delta\beta_0 - \sqrt{2}\kappa$.

If one photon is generated in mode A and the other in mode B, then the value of the phase mismatch will be $\Delta\beta_0 + \sqrt{2}\kappa$.

The quantum entangled state can be manipulated by altering the properties of the input pump laser injected into three waveguides and designing proper κ and L. For example, suppose the SPDC process in the waveguide system to be 775 nm (TM mode) $\to$ 1550 nm (TM mode) + 1550 nm (TM mode) and only the degenerate phase mismatch conditions AA, BC, and CB with the phase mismatch value $\Delta\beta_0$ are excited, which can be ensured to be the proper poling period. When $\kappa > \sqrt{2}\pi/L$, the other phase-matching peaks with phase mismatch $\Delta\beta_0 \pm \sqrt{2}\kappa$ and $\Delta\beta_0 \pm 2\sqrt{2}\kappa$ should be out of the width of $\sin c(\Delta\beta_0 L/2)$. To give the typical parameters in the system, we simulate the waveguide coupling with RSoft software. Suppose the waveguide length is 1 cm. A standard technique is chosen with titanium of thickness 120 nm, a diffusion temperature of $1050\,°C$, and a diffusion time of 5 h. The width of the waveguide is 7.5 μm for ensuring the single-mode condition for the down-converted photons. The distance between waveguides is 12.96 μm, which satisfies the weak-coupled approximation described by the coupled-mode theory, and the coupling coefficient for the down-converted photons is evaluated to be 4.45 cm^{-1}, while the coupling coefficient of the pump is less than 1.5 m^{-1}, which indicates the coupling within 1 cm is definitely negligible.
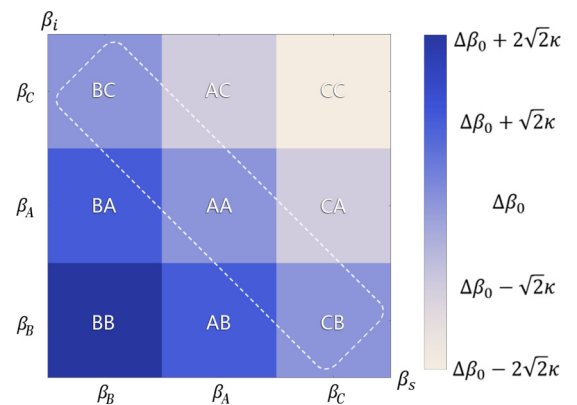

FIG. 2. Combination of different eigenmodes for the signal and the idler photons. The values of phase mismatch are determined by the combination of different eigenmodes.

For simplicity, the amplitude of the pump laser that is injected into the waveguide 1 is considered to be unitary, and the inputs into waveguides 2 and 3 are $\alpha e^{i\theta}$ and $\gamma e^{i\phi}$, respectively. The three amplitudes should be normalized by $\frac{1}{\sqrt{(1+\alpha^2+\gamma^2)}}$, so that the total pump power is assumed to be a constant whose SPDC efficiency will be easily compared with the SPDC from a single waveguide with the same pump power. Then the excitation amplitude of the pump light field in different modes can be written as

$$A_A^{(p)} = \frac{1}{\sqrt{2(1+\alpha^2+\gamma^2)}}(1 - \gamma e^{i\phi}),$$

$$A_B^{(p)} = \frac{1}{2\sqrt{1+\alpha^2+\gamma^2}}(1 + \gamma e^{i\phi} + \sqrt{2}\alpha e^{i\theta}), \tag{12}$$

$$A_C^{(p)} = \frac{1}{2\sqrt{1+\alpha^2+\gamma^2}}(1 + \gamma e^{i\phi} - \sqrt{2}\alpha e^{i\theta}).$$

If we substitute Eqs. (9) and (12) into Eq. (11) and consider the contribution of $\Delta\beta_0$ from the degenerate modes AA, BC, and CB, we can obtain the two-photon state in the eigenmode basis which can also be rewritten in the waveguide basis as

$$|\phi\rangle = U\Phi_0 \iint d\omega_s d\omega_i \alpha(\omega_p)\frac{1}{\sqrt{1+\alpha^2+\gamma^2}}\left\{\frac{1}{2}(1+\gamma e^{i\phi})\sin c\left(\frac{\Delta\beta_0 L}{2}\right)\hat{a}_A^\dagger\hat{a}_A^\dagger + \frac{1}{2}[1+\gamma e^{i\phi} - 2\alpha e^{i\theta}]\sin c\left(\frac{\Delta\beta_0 L}{2}\right)\hat{a}_B^\dagger\hat{a}_C^\dagger\right\}|0\rangle$$

$$= U\Phi_0 \iint d\omega_s d\omega_i \alpha(\omega_p)\frac{1}{\sqrt{1+\alpha^2+\gamma^2}}\left\{\frac{1}{8}(3 + 3\gamma e^{i\phi} - 2\alpha e^{i\theta})(\hat{b}_1^\dagger\hat{b}_1^\dagger + \hat{b}_3^\dagger\hat{b}_3^\dagger)\right.$$

$$\left. -\frac{1}{4}(1+\gamma e^{i\phi} + 2\alpha e^{i\theta})\hat{b}_1^\dagger\hat{b}_3^\dagger - \frac{1}{4}(1+\gamma e^{i\phi} - 2\alpha e^{i\theta})\hat{b}_2^\dagger\hat{b}_2^\dagger\right\}|0\rangle. \tag{13}$$

From the above equation, treating three interactive waves as monochromatic ones, we can see that some special types of two-photon states can be generated only by tuning the condition of pump injection. When waveguides 1, 2, and 3 are excited with the same amplitude of the input laser beam, but with a relative phase of π in waveguide 2, i.e., $\sin c(\frac{\Delta\beta_0 L}{2}) = 1$, $\alpha e^{i\theta} = -1$, $\gamma e^{i\phi} = 1$, the biphoton bunching state will be obtained at the output when normalization is performed, which can be simply described as a two-photon three-path W state:

$$|\phi_1\rangle = \frac{1}{\sqrt{6}}(\hat{b}_1^\dagger\hat{b}_1^\dagger - \hat{b}_2^\dagger\hat{b}_2^\dagger + \hat{b}_3^\dagger\hat{b}_3^\dagger)|0\rangle$$

$$= \frac{1}{\sqrt{3}}(|200\rangle - |020\rangle + |002\rangle), \tag{14}$$

where $|200\rangle$ indicates the state with two photons in the first path-mode and zero photons in the second and the third modes. The biphoton W state generated in the nonlinear waveguides does not require precise control of the waveguide length L and is therefore robust with respect to moderate fabrication inaccuracies. We just need to choose the right pump light to excite the three waveguides under the condition of degenerate phase mismatch.

In the above paragraphs, we introduced the high-dimensional quantum state for a pair of parametric photons, which always locate in the same waveguide if the degenerated phase mismatch is excited. In the following discussion, we explore the general situation in which all the phase mismatches are taken into consideration. By designing the waveguide system appropriately, a wider possibility for modulating two-photon states can be reached. Typical two-photon states in an eigenmode basis can be described as

$$|\psi\rangle^{\text{eig}} = U\Phi_0 \iint d\omega_s d\omega_i \alpha(\omega_p)\frac{1}{\sqrt{1+\alpha^2+\gamma^2}}\left\{\frac{\sqrt{2}}{2}(1-\gamma e^{i\phi})\left\{\sin c\left[\frac{(\Delta\beta_0 - \sqrt{2}\kappa)L}{2}\right]\hat{a}_A^\dagger\hat{a}_B^\dagger\right.\right.$$

$$\left. + \sin c\left[\frac{(\Delta\beta_0 + \sqrt{2}\kappa)L}{2}\right]\hat{a}_A^\dagger\hat{a}_C^\dagger\right\} + \frac{1}{4}[1+\gamma e^{i\phi} + 2\alpha e^{i\theta}]\left\{\sin c\left[\frac{(\Delta\beta_0 - 2\sqrt{2}\kappa)L}{2}\right]\hat{a}_B^\dagger\hat{a}_B^\dagger\right.$$

$$\left. + \sin c\left[\frac{(\Delta\beta_0 + 2\sqrt{2}\kappa)L}{2}\right]\hat{a}_C^\dagger\hat{a}_C^\dagger\right\} + \frac{1}{2}(1+\gamma e^{i\phi})\sin c\left(\frac{\Delta\beta_0 L}{2}\right)\hat{a}_A^\dagger\hat{a}_A^\dagger$$

$$\left. + \frac{1}{2}(1+\gamma e^{i\phi} - 2\alpha e^{i\theta})\sin c\left(\frac{\Delta\beta_0 L}{2}\right)\hat{a}_B^\dagger\hat{a}_C^\dagger\right\}|0\rangle. \tag{15}$$

It can also be rewritten and rearranged in the waveguide basis according to Eq. (9). By tuning the complex amplitude and relative phase of the pump, the coupling coefficient, and the phase mismatch, different quantum states can be generated in the three-coupled-waveguide system, including the W state, i.e., the type of bunching state in which a pair of photons stays in the same waveguide, or the Dicke state [32,33], namely, the antibunching state where n photons locate in m different waveguide modes ($n < m$), or their superposition.

By designing the waveguide structure to tune the propagation constants and coupling coefficients, together with varying the properties of the input pump beam, we can produce specific kinds of quantum entanglement states. For instance, we might like to obtain the Dicke state $|\psi_1\rangle$ at the output which can be described in the waveguide basis as

$$|\psi_1\rangle = \frac{1}{\sqrt{3}}(\hat{b}_1^\dagger \hat{b}_2^\dagger + \hat{b}_2^\dagger \hat{b}_3^\dagger + \hat{b}_1^\dagger \hat{b}_3^\dagger)|0\rangle$$

$$= \frac{1}{\sqrt{3}}(|110\rangle + |011\rangle + |101\rangle). \quad (16)$$

This state means there is only one photon that can be detected from two of the three waveguides. By substituting the aiming state into the rewritten form of Eq. (15) in the waveguide basis, we can obtain the conditions which are needed to generate the desired state. For the Dicke state $|\psi_1\rangle$, the conditions include $\Delta\beta_0 L = 7.267$, $\kappa L = 0.884$, waveguides 1 and 3 are excited with the same input amplitude, and waveguide 2 is excited with 2 times the amplitude in waveguide 1. Likewise, if $\Delta\beta_0 L = 0$, $\kappa L = 2.221$, and the three waveguides are excited with the same input amplitude, but with a phase difference of π in waveguide 2, the state evolves to the case discussed before with only degenerate phase mismatch are excited, and the path-entangled bunching state $|\psi_2\rangle$ can be obtained as

$$|\psi_2\rangle = \frac{1}{\sqrt{3}}(|200\rangle - |020\rangle + |002\rangle). \quad (17)$$

If the conditions of $\Delta\beta_0 L = 5.393$ and $\kappa L = 2.829$ are satisfied, and the input light in waveguide 2 is 0.453 times the amplitudes in waveguides 1 and 3, then the superposition of the W state and the Dicke state can also be obtained as

$$|\psi_3\rangle = \frac{1}{\sqrt{6}}(|200\rangle + |020\rangle + |002\rangle + |110\rangle + |011\rangle + |101\rangle).$$

$$(18)$$

The required conditions for generating certain output states are listed in Table II. We simulate the waveguide coupling with the RSoft software to obtain examples of specific parameters under the same conditions of the poling region length and the wavelength of photons. For instance, when the distance between waveguides is 15.800 μm ($\kappa = 8.839\times10^{-5}$ μm^{-1}), the poling period is 19.085 μm ($\Delta\beta_0 = 7.267\times10^{-4}$ μm^{-1}), the condition in the first line of Table II is satisfied, and $|\psi_1\rangle$ can be generated. Likewise, when the distance between waveguides is chosen to be 14.140 μm ($\kappa = 2.221\times10^{-4}$ μm^{-1}), the poling period is calculated to be 19.043 μm ($\Delta\beta_0 = 0.000$ μm^{-1}) and $|\psi_2\rangle$ can be generated. When the distance between waveguides is 13.730 μm ($\kappa = 2.829\times10^{-4}$ μm^{-1}), the poling period is calculated to be 19.074 μm ($\Delta\beta_0 = 5.393\times10^{-4}$ μm^{-1}) and the generated entangled state is $|\psi_3\rangle$.

TABLE II. The required conditions for generating certain output states. I_1, I_2, and I_3 are the complex amplitudes of the laser beam input into waveguides 1, 2, and 3, respectively.

Complex amplitude	$\Delta\beta_0 L$	κL	Output state
$I_1 = 1/\sqrt{6}$ $I_2 = 2/\sqrt{6}$ $I_3 = 1/\sqrt{6}$	7.267	0.884	$|\psi_1\rangle$
$I_1 = 1/\sqrt{3}$ $I_2 = -1/\sqrt{3}$ $I_3 = 1/\sqrt{3}$	0.00	2.221	$|\psi_2\rangle$
$I_1 = 1/1.485$ $I_2 = 0.453/1.485$ $I_3 = 1/1.485$	5.393	2.829	$|\psi_3\rangle$

Furthermore, we analyzed the dependence of those output states under different excitation parameter conditions in Fig. 3. Taking the entangled state $|\psi_3\rangle$ as an example, we assume that the length of the waveguides is fixed at 1 cm, and the pump amplitude and the phase coupled into waveguides 1 and 3 stay the same. Figures 3(a) and 3(b) illustrate the influence of the input pump amplitude and the relative phase in waveguide 2, respectively. We can see from the figures that several terms in $|\psi_3\rangle$ have the same probability when the amplitude is 0.453 times that in waveguide 1 and with the same phase. Figures 3(c) and 3(d) show the influence of the coupling coefficient and the phase mismatch on the generated output states, respectively. The probabilities of $|200\rangle$ and $|002\rangle$ follow the same tendency because of the symmetry in the coupled-waveguide system, as well as for $|110\rangle$ and $|011\rangle$. In Figs. 3(a) and 3(b), the probabilities of $|110\rangle$ and $|011\rangle$ also follow the same tendency as $|101\rangle$.

For the practical implementations, compensation can be made by adjusting different parameters in the system.
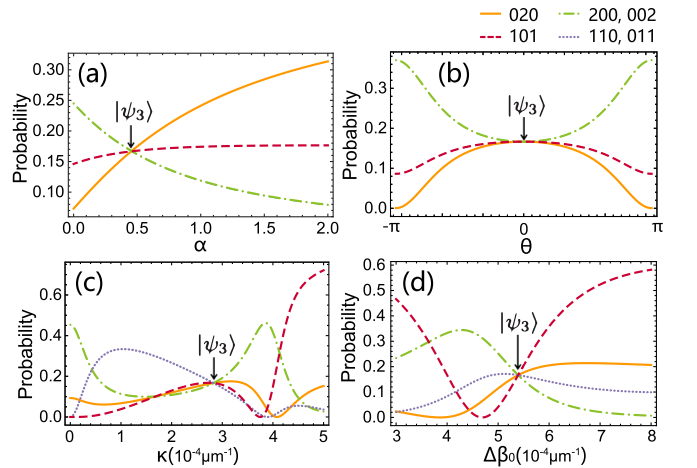
FIG. 3. Relationships between the generated state and the excitation parameters. [(a), (b)] The probabilities of different terms in $|\psi_3\rangle$ vary with the input pump amplitude in waveguide 2 and the phase difference, respectively. [(c), (d)] The probabilities of different terms in $|\psi_3\rangle$ vary with the coupling coefficient and the phase mismatch, respectively.

Amplitudes and phases of the pump can be precisely set through varying the voltages in Mach-Zehnder interferometers of the pump multiplexer. The coupling coefficient can be optimized by a set of different coupling gaps which can be designed on the same chip. The phase-matching condition can be controlled by properly engineering the poling period. For example, the cascaded poling periods can be designed on a single chip to satisfy different requirements. In addition, the tuning of the pump wavelength within its tuning range and the working temperature of the chip can both work as an accessorial skill to mainly refine the coupling coefficient and the phase mismatch, respectively.

When taking several phase mismatches into consideration simultaneously, flexible modulation of entangled states can be realized at the cost of photon pair yield reduction. We estimated the generation rate of these biphoton states, compared with the situation when the QPM SPDC happens inside a single waveguide with the same pump power. After taking the modular square of the amplitude before each quantum state derived from Eq. (15) under the conditions in Table II, the photon pair yield of $|\psi_1\rangle$ will be reduced to 6.76%, and $|\psi_3\rangle$ will be reduced to 16.59%. $|\psi_2\rangle$ is generated under phase-matching conditions and thus is free of the photon pair yield reduction. Since a Ti-diffusion or proton-exchange LN waveguide will enhance the SPDC efficiency by $3 \sim 4$ orders when compared with bulk crystals [9,34], the on-chip generation of path-entangled states is still an advantageous method for the initial quantum state preparation.

When we try to generalize this method to four or more parallel coupled waveguides, we find that the number of control parameters grows slowly when new waveguides are introduced, although the nonuniform gaps can be introduced as new parameters while the dimension of the path-entangled state grows more quickly. Therefore manipulation of path-entangled states seems difficult when the number of waveguides is higher than three.

IV. QUANTIFICATION OF HIGH-DIMENSIONAL ENTANGLEMENT

In order to quantify the degree of entanglement, we calculate the genuine multipartite entanglement (GME) concurrence [35,36] for high-dimensional path-entangled states. For n-partite pure states $|\psi\rangle$ in finite-dimensional Hilbert space $H_i (i = 1, 2, \ldots, n)$, the GME concurrence can be defined as

$$C_{\mathrm{GME}}(|\psi\rangle) = \min_{\gamma_i \in \gamma} \sqrt{2\left[1 - \mathrm{Tr}\rho_{A_{\gamma_i}}^2\right]}, \qquad (19)$$

where $\gamma = \{\gamma_i\} = \{A_{\gamma_i}|B_{\gamma_i}\}$ represents the set of all possible bipartitions, ρ is the density matrix, and the reduced density matrix is written as $\rho_A = \mathrm{Tr}_B\rho$. The GME concurrence can also be generalized for mixed states $\rho = \Sigma_i p_i |\psi_i\rangle\langle\psi_i|$ via a convex roof construction. In the case of three-waveguide system, high-dimensional entangled states $|\psi\rangle \in H_1 \otimes H_2 \otimes H_3$, there are three possible bipartitions, i.e., $\gamma = \{\gamma_1, \gamma_2, \gamma_3\} = \{\{1|2, 3\}, \{2|1, 3\}, \{3|1, 2\}\}$. Consequently, the GME concurrence is $C_{\mathrm{GME}}(|\psi\rangle) = \min\{\sqrt{2[1-\mathrm{Tr}(\rho_1^2)]}$, $\sqrt{2[1 - \mathrm{Tr}(\rho_2^2)]}$, $\sqrt{2[1 - \mathrm{Tr}(\rho_3^2)]}\}$, where ρ_i $(i = 1, 2, 3)$
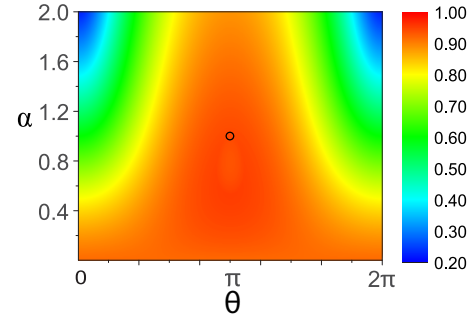

FIG. 4. The dependence of GME concurrences on the pump phase θ and the amplitude α of waveguide 2.

are the reduced density matrices which are taken over all possible decompositions of ρ.

The general form of biphoton high-dimensional entangled states produced in Sec. III can be written as

$$|\psi\rangle = a|110\rangle + b|011\rangle + c|101\rangle$$
$$+ d|200\rangle + e|020\rangle + f|002\rangle, \qquad (20)$$

where a–f represent the coefficients of each term, and the coefficients satisfy the normalization condition $|a|^2 + |b|^2 + |c|^2 + |d|^2 + |e|^2 + |f|^2 = 1$. The density matrix can be obtained by using the equation $\rho = |\psi\rangle\langle\psi|$. Tracing out the subsystem, the reduced density matrices ρ_1, ρ_2, and ρ_3 will be obtained. Therefore, we can get the GME concurrences of certain states by definition. For instance, in the case of the Dicke state $|\psi_1\rangle$, we have $|a| = |b| = |c| = \frac{1}{\sqrt{3}}$ and $|d| = |e| = |f| = 0$; then we can obtain the GME concurrences $C = 2\sqrt{2}/3$. In the case of $|\psi_2\rangle$, $|a| = |b| = |c| = 0$ and $|d| = |e| = |f| = \frac{1}{\sqrt{3}}$; then we can obtain the same GME concurrences. For the state $|\psi_3\rangle = (|200\rangle + |020\rangle + |002\rangle + |110\rangle + |101\rangle + |011\rangle)/\sqrt{6}$, i.e., in the case of the maximal entangled state, the GME concurrences $C = \sqrt{11}/3$.

Furthermore, we analyzed the GME concurrences of entangled states when tuning the typical parameters in the coupled-waveguide system. Since there are many parameters involved, we can only discuss the dependence of GME concurrences on two parameters when the other parameters are selected at some fixed values. Taking the parameters of the W state $(|\psi_2\rangle)$ as an example, we can adjust the amplitude and the phase of the input pump light while the coupling coefficient and the length of the waveguides are fixed. The result of GME concurrences is illustrated in Fig. 4, the horizontal axis and the vertical axis represent the pump phase θ and the amplitude α in waveguide 2, respectively. As we can see from the figure, when the pump input of waveguide 2 shares the same amplitude with the other two waveguides but with a phase difference π, i.e., $\alpha = 1$ and $\theta = \pi$, the entangled state $|\psi_2\rangle$ with the GME concurrences $C = 2\sqrt{2}/3$ can be generated. The relationship between the degree of entanglement and other parameters can also be analyzed in the same way, we do not cover all of them here.

V. CONCLUSION

In conclusion, we investigated the fundamental physics for the generation of a high-dimensional path-entangled state

in quadratic nonlinear coupled-waveguide structures. Photon pairs can be generated through SPDC processes and simultaneously spread through quantum walks in the integrated waveguide chip. We have shown how to harness the path degree of freedom in integrated circuits for engineering high-dimensional biphoton entangled states in multiple channels. The type of entanglement can be manipulated entirely classically by varying the properties of the input pump beam or the phase-matching conditions. Our approach allows for phase-stable state preparation which is free of precise fabrication of the waveguide length. Our path-entangled source extends earlier investigations focusing on waveguide systems which contain two or infinite coupled waveguides. It also simplifies the complexity of integration, as the state preparation is already integrated in the source design and does not need any postprocessing by additional linear circuits. Moreover, combining the state generation with the action of quantum walk in photonic circuits will take the integration density to a different level. These advantages open new perspectives in the field of integrated quantum optics.

[1] J. W. Pan, Z. B. Chen, C. Y. Lu, H. Weinfurter, A. Zeilinger, and M. Zukowski, Multiphoton entanglement and interferometry, Rev. Mod. Phys. **84**, 777 (2012).

[2] R. Fickler, R. Lapkiewicz, M. Huber, M. P. J. Lavery, M. J. Padgett, and A. Zeilinger, Interface between path and orbital angular momentum entanglement for high-dimensional photonic quantum information, Nat. Commun. **5**, 4502 (2014).

[3] Y. B. Zhan, Q. Y. Zhang, Y. W. Wang, and P. C. Ma, Schemes for teleportation of an unknown single-qubit quantum state by using an arbitrary high-dimensional entangled state, Chin. Phys. Lett. **27**, 010307 (2010).

[4] M. Malik, M. Erhard, M. Huber, M. Krenn, R. Fickler, and A. Zeilinger, Multi-photon entanglement in high dimensions, Nat. Photon. **10**, 248 (2016).

[5] A. Rossi, G. Vallone, A. Chiuri, F. De Martini, and P. Mataloni, Multipath Entanglement of Two Photons, Phys. Rev. Lett. **102**, 153902 (2009).

[6] M. Kues, C. Reimer, P. Roztocki, L. R. Cortés, S. Sciara, B. Wetzel, Y. Zhang, A. Cino, S. T. Chu, B. E. Little, D. J. Moss, L. Caspani, J. Azaña, and R. Morandotti, On-chip generation of high-dimensional entangled states and their coherent control, Nature (London) **546**, 622 (2017).

[7] A. C. Dada, J. Leach, G. S. Buller, M. J. Padgett, and E. Andersson, Experimental high-dimensional two-photon entanglement and violations of generalized Bell inequalities, Nat. Phys. **7**, 677 (2011).

[8] J. W. Silverstone, D. Bonneau, K. Ohira, N. Suzuki, H. Yoshida, N. Iizuka, M. Ezaki, C. M. Natarajan, M. G. Tanner, R. H. Hadfield, V. Zwiller, G. D. Marshall, J. G. Rarity, J. L. O'Brien, and M. G. Thompson, On-chip quantum interference between silicon photon-pair sources, Nat. Photon. **8**, 104 (2014).

[9] H. Jin, F. M. Liu, P. Xu, J. L. Xia, M. L. Zhong, Y. Yuan, J. W. Zhou, Y. X. Gong, W. Wang, and S. N. Zhu, On-Chip Generation and Manipulation of Entangled Photons Based on Reconfigurable Lithium-Niobate Waveguide Circuits, Phys. Rev. Lett. **113**, 103601 (2014).

[10] A. Politi, M. J. Cryan, J. G. Rarity, S. Yu, and J. L. O'Brien, Silica-on-silicon waveguide quantum circuits, Science **320**, 646 (2008).

[11] S. L. Mouradian, T. Schröder, C. B. Poitras, L. Li, J. Goldstein, E. H. Chen, M. Walsh, J. Cardenas, M. L. Markham, D. J. Twitchen, M. Lipson, and D. Englund, Scalable Integration of Long-Lived Quantum Memories into a Photonic Circuit, Phys. Rev. X **5**, 031009 (2015).

[12] F. Najafi, J. Mower, N. C. Harris, F. Bellei, A. Dane, C. Lee, X. L. Hu, P. Kharel, F. Marsili, S. Assefa, K. K. Berggren, and D. Englund, On-chip detection of non-classical light by scalable integration of single-photon detectors, Nat. Commun. **6**, 5873 (2015).

[13] B. J. Metcalf, J. B. Spring, P. C. Humphreys, N. Thomas-Peter, M. Barbieri, W. S. Kolthammer, X. M. Jin, N. K. Langford, D. Kundys, J. C. Gates, B. J. Smith, P. G. R. Smith, and I. A. Walmsley, Quantum teleportation on a photonic chip, Nat. Photon. **8**, 770 (2014).

[14] P. Sibson, C. Erven, M. Godfrey, S. Miki, T. Yamashita, M. Fujiwara, M. Sasaki, H. Terai, M. G. Tanner, C. M. Natarajan, R. H. Hadfield, J. L. O'Brien, and M. G. Thompson, Chip-based quantum key distribution, Nat. Commun. **8**, 13984 (2017).

[15] M. Gräfe, R. Heilmann, A. Perez-Leija, R. Keil, F. Dreisow, M. Heinrich, H. Moya-Cessa, S. Nolte, D. N. Christodoulides, and A. Szameit, On-chip generation of high-order single-photon W-states, Nat. Photon. **8**, 791 (2014).

[16] A. Perez-Leija, J. C. Hernandez-Herrejon, H. Moya-Cessa, A. Szameit, and D. N. Christodoulides, Generating photon-encoded *W* states in multiport waveguide-array systems, Phys. Rev. A **87**, 013842 (2013).

[17] A. Perez-Leija, R. Keil, H. Moya-Cessa, A. Szameit, and D. N. Christodoulides, Perfect transfer of path-entangled photons in J_x photonic lattices, Phys. Rev. A **87**, 022303 (2013).

[18] R. Kruse, F. Katzschmann, A. Christ, A. Schreiber, S. Wilhelm, K. Laiho, A. Gabris, C. S. Hamilton, I. Jex, and C. Silberhorn, Spatio-spectral characteristics of parametric downconversion in waveguide arrays, New J. Phys. **15**, 083046 (2013).

[19] C. S. Hamilton, R. Kruse, L. Sansoni, C. Silberhorn, and I. Jex, Driven Quantum Walks, Phys. Rev. Lett. **113**, 083602 (2014).

[20] A. S. Solntsev, A. A. Sukhorukov, D. N. Neshev, and Y. S. Kivshar, Spontaneous Parametric Down-Conversion and

Quantum Walks in Arrays of Quadratic Nonlinear Waveguides, Phys. Rev. Lett. **108**, 023601 (2012).

[21] A. S. Solntsev, F. Setzpfandt, A. S. Clark, C. W. Wu, M. J. Collins, C. Xiong, A. Schreiber, F. Katzschmann, F. Eilenberger, R. Schiek, W. Sohler, A. Mitchell, C. Silberhorn, B. J. Eggleton, T. Pertsch, A. A. Sukhorukov, D. N. Neshev, and Y. S. Kivshar, Generation of Nonclassical Biphoton States through Cascaded Quantum Walks on a Nonlinear Chip, Phys. Rev. X **4**, 031007 (2014).

[22] R. Kruse, L. Sansoni, S. Brauner, R. Ricken, C. S. Hamilton, I. Jex, and C. Silberhorn, Dual-path source engineering in integrated quantum optics, Phys. Rev. A **92**, 053841 (2015).

[23] C. W. Wu, A. S. Solntsev, D. N. Neshev, and A. A. Sukhorukov, Photon pair generation and pump filtering in nonlinear adiabatic waveguiding structures, Opt. Lett. **39**, 953 (2014).

[24] F. Setzpfandt, A. S. Solntsev, J. Titchener, C. W. Wu, C. Xiong, R. Schiek, T. Pertsch, D. N. Neshev, and A. A. Sukhorukov, Tunable generation of entangled photons in a nonlinear directional coupler, Laser Photon. Rev. **10**, 131 (2016).

[25] F. Setzpfandt, A. S. Solntsev, and A. A. Sukhorukov, Nonlocal splitting of photons on a nonlinear chip, Opt. Lett. **41**, 5604 (2016).

[26] Y. Yang, P. Xu, L. L. Lu, and S. N. Zhu, Manipulation of a two-photon state in a $\chi^{(2)}$-modulated nonlinear waveguide array, Phys. Rev. A **90**, 043842 (2014).

[27] J. Wang, S. Paesani, Y. Ding, R. Santagati, P. Skrzypczyk, A. Salavrakos, J. Tura, R. Augusiak, L. Mančinska, D. Bacco, D. Bonneau, J. W. Silverstone, Q. Gong, A. Acín, K. Rottwitt, L. K. Oxenløwe, J. L. O'Brien, A. Laing, and M. G. Thompson,

Multidimensional quantum entanglement with large-scale integrated optics, Science **360**, 285 (2018).

[28] H. Y. Leng, X. Q. Yu, Y. X. Gong, P. Xu, Z. D. Xie, H. Jin, C. Zhang, and S. N. Zhu, On-chip steering of entangled photons in nonlinear photonic crystals, Nat. Commun. **2**, 429 (2011).

[29] H. Jin, P. Xu, X. W. Luo, H. Y. Leng, Y. X. Gong, W. J. Yu, M. L. Zhong, G. Zhao, and S. N. Zhu, Compact Engineering of Path-Entangled Sources from a Monolithic Quadratic Nonlinear Photonic Crystal, Phys. Rev. Lett. **111**, 023603 (2013).

[30] S. Somekh, E. Garmire, A. Yariv, H. L. Garvin, and R. G. Hunsperger, Channel optical waveguide directional couplers, Appl. Phys. Lett. **22**, 46 (1973).

[31] F. M. Miatto, A. M. Yao, and S. M. Barnett, Full characterization of the quantum spiral bandwidth of entangled biphotons, Phys. Rev. A **83**, 033816 (2011).

[32] M. Bergmann and O. Gühne, Entanglement criteria for Dicke states, J. Phys. A **46**, 385304 (2013).

[33] H. Y. Liu, R. Zhang, P. Xu, Z. D. Xie, Y. X. Gong, and S. N. Zhu, Compact generation of a two-photon multipath Dicke state from a single $\chi^{(2)}$ nonlinear photonic crystal, Opt. Lett. **44**, 239 (2019).

[34] S. Tanzilli, H. De Riedmatten, H. Tittel, H. Zbinden, P. Baldi, M. De Micheli, D. B. Ostrowsky, and N. Gisin, Highly efficient photon-pair source using a periodically poled lithium niobate waveguide, Electron. Lett. **37**, 26 (2001).

[35] F. Mintert, M. Kuś, and A. Buchleitner, Concurrence of Mixed Multipartite Quantum States, Phys. Rev. Lett. **95**, 260502 (2005).

[36] Z. H. Ma, Z. H. Chen, J. L. Chen, C. Spengler, A. Gabriel, and M. Huber, Measure of genuine multipartite entanglement with computable lower bounds, Phys. Rev. A **83**, 062325 (2011).